UC SESM 71-2

STRUCTURES AND MATERIALS RESEARCH
DEPARTMENT OF CIVIL ENGINEERING

ELASTIC - PLASTIC ANALYSIS OF AXISYMMETRIC SOLIDS USING ISOPARAMETRIC FINITE ELEMENTS

P. K. LARSEN
E. P. POPOV

Report to
Army Research Office, Durham
Contract No. DAHCO 4 69 C 0037

JANUARY 1971

STRUCTURAL ENGINEERING LABORATORY
UNIVERSITY OF CALIFORNIA
BERKELEY CALIFORNIA

ELASTIC-PLASTIC ANALYSIS OF AXISYMMETRIC SOLIDS USING ISOPARAMETRIC FINITE ELEMENTS

by

P. K. Larsen
E. P. Popov

Report to the
Army Research Office - Durham
Contract No. DAHCO 4 69C 0037

January 1971

ABSTRACT

Application of special isoparametric finite elements is presented for elastic-plastic analysis of shells of revolution. General isoparametric elements are selected which in the form of a layered system are capable of representing a solid of revolution. The customary Kirchhoff-Love hypothesis is not invoked and the solutions therefore apply both to thin and thick shells of revolution. Sharp discontinuities in geometry, circumferential ribs and/or grooves, as well as cellular walls, may be studied. A special feature is the development of an element permitting sliding at the element interfaces with or without friction. The illustrative examples include a pressure vessel with a circumferential crack in the wall thickness, a circular plate consisting of two discs which can slide along their interface, and shrink-fit of two thick-walled circular cylinders. The solutions are limited to axially symmetric problems. Flow theory of plasticity is used in the inelastic range.

NOMENCLATURE

$[B]$ = strain-displacement transformation matrix

$[C]$ = stress-strain transformation matrix for elastic-plastic deformation

$[E]$ = stress-strain transformation matrix for elastic deformations (generalized Hooke's Law)

E = Young's Modulus

E_t = Tangent Modulus

ν = Poisson's ratio

μ, λ = Lamé constants

r, z = global coordinates

$[J]$ = Jacobian transformation

ψ = field variable

φ_l = interpolation polynomials

ξ, η = natural coordinates

ε_{ij} = infinitesimal strain components

ε_{ij}^{P} = plastic strain components

ε_{ij}^{E} = elastic strain components

$\bar{\varepsilon}^{P}$ = equivalent plastic strain

σ_{ij} = stress components

s_{ij} = deviatoric stress components

$\bar{\sigma}$ = equivalent stress

f = yield (loading) function

κ = hardening parameter

J_2 = second invariant of deviatoric stress tensor

$d\lambda$ = non-negative scalar

H = hardening function

δ_{ij} = Kronecker delta function

α = loading parameter

TABLE OF CONTENTS

1. INTRODUCTION

A computer program using isoparametric elements for elastic-plastic analysis of axisymmetric thick-walled shells has been written. The main purpose of the program is to determine the overall behavior and ultimate load for shells with sharp discontinuities in wall thickness. For detailed information about local stress and strain distribution around the discontinuities a very fine finite element mesh has to be used, for which the program is uneconomical.

A series of elements specially suited for analysis of thick shells were selected from the family of isoparametric elements, and a noncompatible version of these elements was investigated in order to reduce the band-width of the stiffness matrix.

The possibility of sliding interfaces between elements has been introduced, and friction at this interface is included, either represented by discrete springs or by Coulomb's friction.

Flow theory of plasticity has been used in the inelastic analysis, and a short review of this theory has been included. The efficiency of highly refined elements in elastic-plastic analysis was also studied.

2. ISOPARAMETRIC FINITE ELEMENTS

2.1 Compatible Elements

The isoparametric family of finite elements is among the most effective elements developed recently [1]. This family of elements allows large flexibility in choice of element to fit geometry and continuity requirements on the displacement field. The present presentation gives a short review of the theoretical background pertinent to the choice of element type in an elastic-plastic analysis of thick-walled shells with sharp discontinuities in wall thickness.

On a general quadrilateral in a two-dimensional space with or without curved sides, any field variable can be approximated by

$$\Psi = \sum_{i=1}^{N} \varphi_i(\xi, \eta)\ \Psi_i \tag{2-1}$$

where φ_i are interpolation polynomials in terms of the natural coordinates ξ and η, and Ψ_i are the nodal point values of the variable. The number of nodes and the order of the polynomials are determined by the shape of the domain and the continuity requirements on Ψ.

The basic concept of the isoparametric element is the choice of the same interpolation formula for both the geometry and the displacement field of the element

$$\begin{Bmatrix} r \\ z \end{Bmatrix} = \sum_{i=1}^{N} \varphi_i(\xi, \eta) \begin{Bmatrix} r_i \\ z_i \end{Bmatrix} \tag{2-2}$$

$$\begin{Bmatrix} u \\ v \end{Bmatrix} = \sum_{i=1}^{N} \varphi_i(\xi, \eta) \begin{Bmatrix} u_i \\ z_i \end{Bmatrix} \tag{2-3}$$

where (r_i, z_i) and (u_i, v_i) are the nodal point coordinates and displacements, respectively. This choice completely defines the geometry of the element, and includes the constant straining and rigid body modes. A natural extension of this concept is to use a higher order approximateion for the displacements than for the geometry [2]. In section 2.2 another variation of the basic concept is used, where an incompatible displacement mode is added.

For the particular application at hand, the shape of the element and the differentiability of the displacement field must be decided upon apriori. In a shell type structure an accurate representation of the geometry may be necessary, and the most suitable elements for such application are given in Fig. 1. Besides the requirement on representation of geometry, the order of the polynomials $\varphi_i(\xi, \eta)$ is mainly determined by the following considerations:

For simulation of flexural behavior, at least a linear variation of curvature in the ξ-direction should be included. This implies that φ_i should be at least of order three in ξ. In a pure bending mode a lower order polynomial would give excessive strain energy associated with shear deformation. This problem has been avoided by Doherty, et al. [3] by using different integration points for the numerical evaluation of the energy associated with bending and of that with shear. For elastic-plastic analysis, however, this approach is not easily applicable due to the progressive yielding in the element.

In order to reduce the band-width and number of equations, the

minimum number of nodes in the η-direction must be used. A linear variation of displacements in this direction, (NP8-1), gives for a rectangular element a constant ϵ_η strain component. In the thin shell theory such a restriction on the displacement field is immaterial since ϵ_η is not a primary kinematic variable, but is rather determined from constitutive theory. However, using this assumption in a thick-shell approach gives for pure bending errors in the order of 10-15% in the displacements. The reason for this is that in pure bending Hooke's law gives $\epsilon_\eta = - \nu\epsilon_\xi$, i.e., linear variation in η, and the formulation of the problem using variational principles gives excessive energy in the element when the assumed displacement field is incompatible with the actual one. Except for materials where Poisson's ratio equals zero, the linear variation in the displacement field in the η-direction is therefore insufficient. It should be further noted that in elastic-plastic deformation part of the element may be plastic, and hence ϵ_η may actually be discontinuous within the element.

The above considerations are illustrated by the analysis of a circular plate under uniform loading, Fig. 2. In the actual analysis only half the plate thickness was considered, and boundary conditions were applied at the middle surface. The transverse displacement and stresses, normalized with respect to the Timoshenko solution, is given in Tables I-IV.

Of the two compatible elements, (NP8-1) and (NP10), the latter is the superior one and is chosen as the basic element. The merits of the incompatible element (NP8-3) will be discussed in the next section. For structures where the elements are only connected in the

TABLE I

Transverse Displacement v/v_o

r/a	0.0	0.25	0.50	0.75
NP8-1	0.9269	0.9270	0.9263	0.8974
NP10	0.9994	0.9961	1.000	0.9695
NP8-3	1.0257	1.0274	1.0293	1.0000

TABLE II

Radial Stress σ_r/σ_r^o

r/a	0.0	0.0833	0.1666	0.25	0.50	0.75
NP8-1	1.0937	1.0910	1.0912	1.0946	1.0995	1.0872
NP10	1.0022	1.0011	1.0006	1.0024	1.0037	0.9987
NP8-3	0.9602	0.9819	0.9942	1.0024	1.0150	1.0192

TABLE III

Hoop Stress $\sigma_\theta/\sigma_\theta^o$

r/a	0.0	0.0833	0.1666	0.25	0.50	0.75
NP8-1	1.0937	1.0913	1.0895	1.0891	1.0786	1.0498
NP10	1.0022	1.0017	1.0011	1.0012	1.0007	0.9992
NP8-3	0.9602	0.9763	0.9857	0.9965	1.0098	1.0199

TABLE IV

Vertical Stress σ_z/q

r/a	0.0	0.0833	0.1666	0.25	0.50	0.75
NP8-1	66.9	66.4	65.2	63.5	53.4	36.0
NP10	0.6	0.1	0.3	0.3	0.4	0.7
NP8-3	12.4	11.5	11.8	9.6	7.2	4.2

ξ-direction (NP10) gives a reasonable band-width. However, for sandwich shells and shells with sharp discontinuities in the thickness, several elements must be used over the thickness. In such cases it may be advantageous to convert from using a two-layered system to one of one layer, by a combination of the elements shown in Fig. 1. It should, however, be noted that by connecting one element with a quadratic displacement field to two elements with a linear displacement field, continuity is only obtained in a restricted sense.

2.2 Incompatible Element

In order to reduce the band-with compared to element (NP10), an incompatible element (NP8-3) was investigated. This element is similar to element (NP8-1), except that an incompatible displacement mode is added [4]. This additional mode is given by

$$\begin{Bmatrix} u \\ v \end{Bmatrix} = \varphi_\alpha(\xi,\eta) \begin{Bmatrix} u_\alpha \\ v_\alpha \end{Bmatrix} \quad \text{no summation on } \alpha \tag{2-4}$$

with

$$\varphi_\alpha(\xi,\eta) = \tfrac{1}{2}(1 - \eta^2) \tag{2-5}$$

u_α and v_α are internal degrees of freedom that are condensed out by static condensation before the element stiffness is assembled into the system stiffness. This displacement mode is incompatible along the element sides $\xi = \pm 1$. However, it improves the behavior of the element as seen from Tables I-IV.

This element was, however, not chosen as the basic one due to the relatively high σ_z stresses in the above example. For elastic-plastic analysis these stresses might well initiate premature yielding.

3. INCREMENTAL THEORY OF PLASTICITY

The theory of plasticity is usually divided into two subclasses, the flow theory and the deformation theory. The deformation (or Hencky) theory gives a relationship between total stress and strain, where the total plastic strain components are a function of the current stress. This approach is similar to the treatment of nonlinear elasticity, except for the inclusion of the concept of elastic unloading from the plastic region. The flow theory, on the other hand, is an incremental theory that gives a relationship between increments of plastic strain and increments of stress. Whereas the former is independent of the loading path, the latter has to be integrated along the loading path in order to get the total strains. For proportional or radial loading, i.e., where the ratios between the stress components are kept constant during the deformation, it can be shown that the two theories give the same result. However, for non-radial loading the flow theory is considered the superior one, and is therefore chosen in this study.

In the flow theory the behavior of a structure is governed by three conditions:

i) The initial yield condition

ii) The flow rule

iii) The hardening rule

Although many mathematical forms have been proposed for the initial yield condition, the most general ones express the yield function as a function of the state of stress and a hardening parameter K .

The one most commonly used is von Mises condition, which is given by

$$f = J_2 - K^2 = 0 \tag{3-1}$$

where J_2 is the second invariant of the deviatoric stress tensor, and the hardening factor K is taken as the yield stress in pure shear.

Assuming the existence of a plastic potential, g, the flow rule gives the plastic strain increment as

$$d\epsilon_{ij}^P = d\lambda \frac{\partial g}{\partial \sigma_{ij}} \tag{3-2}$$

where $d\lambda$ is a non-negative scalar. In most cases the potential g is taken to be identical to the yield function f.

The yield condition (3-1) can in a more general form be given as a function of stress and plastic strain. Using the isotropic hardening rule which predicts a uniform expansion of the initial yield function with increasing stresses, one has

$$f = f(J_2) - H(\bar{\epsilon}^P) = 0 \tag{3-3}$$

Here $H(\bar{\epsilon}^P)$ is a function of effective plastic strain, and gives a measure of the strain hardening.

During loading from one plastic state to another the following relation holds

$$df = \frac{\partial f}{\partial \sigma_{ij}} d\sigma_{ij} + \frac{\partial f}{\partial \epsilon_{ij}^P} d\epsilon_{ij}^P = 0 \tag{3-4}$$

From (3-2) and (3-4) one gets [5]

$$d\epsilon_{ij}^P = - \frac{\dfrac{\partial f}{\partial \sigma_{ij}} \dfrac{\partial f}{\partial \sigma_{kl}}}{\dfrac{\partial f}{\partial \epsilon_{mn}^P} \dfrac{\partial f}{\partial \sigma_{mn}}} d\sigma_{kl} \tag{3-5}$$

The generalized Hooke's law is given by

$$d\sigma_{ij} = E_{ijkl}\, d\epsilon^{E}_{kl} = E_{ijkl}\,(d\epsilon_{kl} - d\epsilon^{P}_{kl}) \tag{3-6}$$

with

$$E_{ijkl} = \mu(\delta_{ik}\delta_{jl} + \delta_{il}\delta_{kj}) + \lambda\delta_{ij}\delta_{kl} \tag{3-7}$$

and the Lamé constants

$$\mu = \frac{E}{2(1+\nu)} \qquad \lambda = \frac{\nu E}{(1+\nu)(1-2\nu)}$$

Combining Eqs. (3-2,4,5,6) the incremental stress-strain relationship is found [6]

$$d\sigma_{ij} = C_{ijkl}\, d\epsilon_{kl} \tag{3-8}$$

with

$$C_{ijkl} = E_{ijkl} - \alpha h\, E_{ijmn} \frac{\partial f}{\partial \sigma_{mn}} \frac{\partial f}{\partial \sigma_{rs}} E_{rskl} \tag{3-9}$$

$$h^{-1} = E_{ijkl} \frac{\partial f}{\partial \sigma_{ij}} \frac{\partial f}{\partial \sigma_{kl}} - \frac{\partial f}{\partial \epsilon^{P}_{ij}} \frac{\partial f}{\partial \sigma_{ij}} \tag{3-10}$$

Here α is a loading parameter which is equal to one for loading or neutral loading, and zero for unloading, [6], i.e.,

$$\alpha = 1 \quad \text{if} \quad \frac{\partial f}{\partial \sigma_{ij}}\, d\sigma_{ij} \geq 0$$

$$\alpha = 0 \quad \text{if} \quad \frac{\partial f}{d\sigma_{ij}}\, d\sigma_{ij} < 0 \tag{3-11}$$

Following [6] this can be further simplified to

$$C_{ijkl} = \mu(\delta_{ik}\delta_{jl} + \delta_{il}\delta_{jk}) + \lambda\delta_{ij}\delta_{kl} - \alpha\, 9\mu^2 h \frac{1}{\bar{\sigma}^2}\, S_{ij}S_{kl} \tag{3-12}$$

where

$$\zeta = \frac{E_t}{E}$$

$$h = \frac{2(1 + \nu)(1 - \zeta)}{E[3 - \zeta(1 - 2\nu)]}$$

$$S_{ij} = \sigma_{ij} - \frac{1}{3} \delta_{ij} \sigma_{kk}$$

$$\bar{\sigma} = \sqrt{3J_2}$$

Recalling that in the present study $\epsilon_{13} = \epsilon_{23} = \sigma_{13} = \sigma_{23} = 0$ one can now determine C_{ijkl} and substitute it into the expression for the tangent stiffness matrix.

4. SOLUTION METHOD

The use of the flow theory of plasticity implies that an incremental solution method has to be used. It is, however, well known that such methods have a tendency to diverge from the true solution. Therefore a "one-step iteration" or "out-of-balance force" method was used to counteract this tendency.

For each load increment the variational (or virtual work) method will, in an average sense, give equilibrium between applied external load increment and the increment of internal stress field. For an inelastic analysis, however, equilibrium between total external load and total stress field cannot be expected.

The "one-step iteration" procedure is illustrated in Fig. 3. At the load level R_i the incremental method gives the displacement r_i, while the correct one is r_i^*. The equilibrium load associated with the displacement r_i is R_i^*. For this displacement there exists an out-of-balance force

$$\Delta R_i^* = R_i - R_i^*$$

Having computed the tangent stiffness associated with r_i and R_i, the next load increment is taken as

$$\Delta R_{i+1} = R_{i+1} - R_i^* = R_{i+1} - R_i + \Delta R_i^*$$

The effect of this can be seen in Fig. 3. The pure incremental method will go from point 1 to point 3. The "one-step iteration" method, however, goes from point 0 to point 4 without ever formally updating the displacement or loading for the previous step. The method is illustrated in numerical Example No. 1. The equilibrium nodal load

vector $\{R^*\}$ can easily be found in terms of the total stress field $\{\sigma\}$ by the principle of virtual work

$$\langle \delta u \rangle \{R^*\} = \int_V \langle \delta \epsilon \rangle \{\sigma\} \, dv$$

5. SPECIAL FEATURES

5.1 Sliding Interfaces with Elastic Springs

The finite element idealization of the structure easily accommodates the possibility of a sliding surface within the structure. Such cases might arise in circular plates constructed from two or more layers welded together only around their circumferential boundary, or in shrink fits of axisymmetric structures. The different layers might also be joined together by discrete bolts or screws, the effect of which may be idealized by discrete springs.

A general idealization of a slip-surface is shown in Fig. 4. The local coordinates s and t are tangential and normal to the slip-surface, respectively. Node i of element 1 and node j of element 2 have different global nodal numbers, and are connected with a system of springs.

Defining the displacement $\bar{u}$ and $\bar{v}$ in the local coordinate system s, t, on has the following stiffness relationship:

$$\begin{bmatrix} K_2 & 0 & -K_2 & 0 \\ 0 & K_1 & 0 & -K_1 \\ -K_2 & 0 & K_2 & 0 \\ 0 & -K_1 & 0 & K_1 \end{bmatrix} \cdot \begin{bmatrix} \bar{u}_i \\ \bar{v}_i \\ \bar{u}_j \\ \bar{v}_j \end{bmatrix} = \begin{bmatrix} R_{i1} \\ R_{i2} \\ R_{j1} \\ R_{j2} \end{bmatrix} \qquad (5\text{-}1)$$

or

$$[\bar{K}]\ \{u\} = \{\bar{R}\} \tag{5-2}$$

Since the system stiffness matrix is given in global coordinates, (5-2) must be transformed into

$$[K]\ \{u\} = \{R\} \tag{5-3}$$

where

$$[K] = [A]^T[\bar{K}]\ [A]$$

$$\{R\} = \{\bar{R}\}\ [A]$$

and $[A]$ is the transformation matrix between the local coordinates (s,t), and the global system (r,z).

In the case of an elastic spring acting between the nodes i and j, the spring constants K_1 and K_2 will be given. However, if no such spring exists, but the surfaces are free to slide along each other, K_2 is zero. In most cases there is physical contact between the two elements along the surface, and hence node i and j are free to move apart in the t direction, but cannot move together. Thus an iterative or incremental approach has to be used, in which the spring constant K_1 is assigned the value zero if the normal stress across the surface is positive, and an infinite value otherwise. Numerically the latter might be obtained by either assigning $\bar{v}_1 = \bar{v}_j$ as boundary condition

and modifying the system stiffness matrix accordingly, or simply assigning K_1 the value of the diagonal element associated with node i in the system stiffness matrix, multiplied by a large number, say 10^6. For most practical purposes this has the same effect, and the latter method is chosen in the program.

5.2 Sliding Interfaces with Friction

In structures with sliding interfaces, as above, we may wish to include the effect of friction between the two layers. Friction gives rise to energy dissipation in the form of heat, and hence the principle of minimum potential energy is not valid. However, a virtual work expression can readily be written of the form

$$\int_V \sigma_{i,j}\,\delta\epsilon_{i,j}\,dV + \alpha \int_\Gamma |\hat{t}_i\,\delta\hat{u}_i|\,d\Gamma = \int_A P_i\,\delta u_i\,dA \qquad (5\text{-}4)$$

Here body forces are for simplicity assumed absent. Γ is the surface over which friction takes place, and $\hat{\underset{\sim}{t}}$ and $\delta\hat{\underset{\sim}{u}}$ are respectively the traction and the relative virtual displacement tangential to Γ. A friction parameter α takes on the value of one when friction takes place, and the value of zero otherwise. Equation (5-4) is actually a statement of energy balance, i.e., applied external work is equal to strain energy stored in the system and friction energy dissipated. The traction $\hat{t}$ takes on the role as an initial stress, and can easily be converted to a fictitious external load in the equilibrium equations.

The traction $\hat{\underset{\sim}{t}}$ tangential to the surface is given by

$$\hat{\underset{\sim}{t}}(\xi) = \tau_{\eta\xi}(\xi)\,d\Gamma \qquad (5\text{-}5)$$

$$d\Gamma = 2\pi r(\xi) \sqrt{\left(\frac{\partial r}{\partial \xi}\right)^2 + \left(\frac{\partial z}{\partial \xi}\right)^2}\, d\xi \qquad (5\text{-}6)$$

For simplicity let τ denote $\tau_{\eta\xi}$, and τ_i the value of $\tau_{\eta\xi}$ at the nodal points of the sliding surface.

By interpolation

$$\tau(\xi) = \varphi_i(\xi)\tau_i \quad , \quad i = 1,4 \qquad (5\text{-}7)$$

Let u_{1i} and u_{2i} denote the nodal displacements of node i in element 1 and 2 respectively

$$\hat{\delta u} = \langle \cos\Psi \ \sin\Psi \ - \cos\Psi \ - \sin\Psi \rangle \begin{bmatrix} \Phi & 0 \\ 0 & \Phi \end{bmatrix} \begin{Bmatrix} \delta u_{11} \\ \delta v_{11} \\ \vdots \\ \delta v_{24} \end{Bmatrix} \qquad (5\text{-}8)$$

where

$$\Phi = \begin{bmatrix} \varphi_1 & 0 & \varphi_2 & 0 & \varphi_3 & 0 & \varphi_4 & 0 \\ 0 & \varphi_1 & 0 & \varphi_2 & 0 & \varphi_3 & 0 & \varphi_4 \end{bmatrix} \qquad (5\text{-}9)$$

From these equations the "equivalent" loading can be given as:

$$\langle R_f \rangle = \delta \cdot \alpha \cdot \int_\Gamma \tau(\xi) \ \langle \cos\Psi \ \sin\Psi \ - \cos\Psi \ - \sin\Psi \rangle \begin{bmatrix} \Phi & 0 \\ 0 & \Phi \end{bmatrix} d\Gamma \qquad (5\text{-}10)$$

Friction will now take place whenever $\tau_{\eta\xi} \geq \mu\sigma_{\eta\eta}$ and simultaneously $\sigma_{\eta\eta} < 0$, where μ is a coefficient of friction. Due to the necessity of testing on friction, the solution has to be found incrementally, where the present stress ratio will determine the value of α for the next load increment. The parameter δ determines the sign of $\{R_f\}$ according to the sign of the relative displacement between the two elements at the previous load increment.

6. NUMERICAL EXAMPLES

6.1 Elastic-Plastic Analysis of Simply Supported Beam

This example is included in order to illustrate the effect of the "one-step iteration" procedure. A simply supported beam shown in Fig. 5 was analyzed using both the pure incremental and the "one-step iteration" method, and compared to the exact solution [7]. A total of 11 load increments was used. As can be seen from the normalized load-deflection curves in Fig. 5, the improvement in convergence is substantial, allowing larger step size to be used. The additional computational effort is negligible.

6.2 Elastic-Plastic Analysis of Imperfect Torispherical Head

A torispherical head with radial circumferential crack half way through the wall thickness was studied. The overall behavior and ultimate strength of this pressure vessel is compared with a similar uncracked shell. No attempt was made to investigate the local stress and strain distribution in the immediate neighborhood of the crack. Such a study would require a very fine finite element mesh at the root of the crack, and would involve the theory of fracture mechanics. For this study the material was assumed to be ductile enough to accommodate the plastic strains at the tip of the crack without local fracture.

The torispherical head has a skirt diameter, $D = 100$ in., the radius of the sphere $R = D$, the meridional radius of the torus $r = 0.2D$, and the uniform shell thickness $h = 0.02\ D$. The material is assumed to be elastic-perfectly plastic with yield stress $\sigma_y = 3 \times 10^4$ psi, and Young's modulus and Poisson's ratio 3×10^7 psi and 0.3, respectively.

The radial crack is located at the junction between the sphere and

the torus, which is the region of highest meridional moment. The crack is on the inner face at the shell. On the basis of an elastic analysis the stresses both for the cracked and uncracked head is obtained, Fig. 6. As can be seen, the effect of the crack is restricted to the region immediately around the crack, and the stress increase locally is approximately 70%. In spite of this stress increase, the ultimate load for the cracked shell is only reduced by 6%, Fig. 7. The propagation of elastic-plastic boundaries is shown in Fig. 8. As can be seen, the crack initiates the formation of a plastic zone at the root of the crack, but this zone does not significantly alter the final collapse mechanism.

Both shells were analyzed using 32 elements, arranged in two layers over the thickness. In the region closest to the crack 16 Gauss points were used over the shell thickness, while 8 points were used in the remaining part of the shell.

6.3 Elastic-Plastic Analysis of Layered Circular Plate

A circular plate constructed of two discs welded together along their outer boundary was analyzed. The diameter of the plate is 48 in., and the thickness of each disc is 3 in. The plate is loaded by a ring load, and the material properties were assumed to be the same as in the previous example. The analysis shows that welding along the outer boundary introduces a distributed radial moment along the boundary in order to maintain compatibility between the discs. This can be seen from Fig. 9, where the vertical deflection along a radius is plotted both for a homogeneous and a layered plate. The load-deflection curves are given in Fig. 10, where the normalizing factors are the load and deflection at initial yielding for the respective homogeneous plates.

6.4 Shrink-Fit of Two Cylindrical Discs

The analysis of shrink-fit problems is illustrated by a case where two cylindrical discs are joined together. This class of problems can be solved by two different methods:

1. The two parts are connected with discrete springs at the interface where the parts are to be joined together. The stiffness of these springs should be "large" compared to the elements of the system stiffness matrix. At either end of the springs a self-equilibrating set of forces should be applied. The magnitude of these forces should be such that they produce a displacement in the springs that is equal to the difference between the radii of the two parts being assembled.

   In the present case the stiffness of the springs was varied between 10^8 and 10^{16} without any significant change in the results. Larger values, however, gave numerical problems and inaccurate results.

2. The alternative method is to prescribe such displacement in either the inner or outer disc so that the two parts fit together and to connect the two parts. Then the whole system is released and it will return to an equilibrium position.

Numerically, the first method is superior, since the problem can be solved directly, while the second method solves the problem in two steps. For elastic systems the two methods give identical results. However, if the difference in radii between the two parts is large, the second method may result in plastic deformations during step one, and the final state of stress will include large residual stresses. The

method of superposition does not apply to inelastic cases. This is illustrated by a numerical example. The inner disc has radii of 6.0 in. and 8.0 in., and the outer one has radii 7.9 in. and 9.9 in. The thickness of both discs is 1.0 in. Method 1 gives results that are identical to Timoshenko's classical solution, while method 2 gives large residual stresses and different displacements, Fig. 11. The stresses are normalized with respect to the radial and hoop stress at the inner face of the outer disc.

7. CONCLUSION

An effective program for elastic-plastic analysis of axisymmetric thick-walled shells using isoparametric elements has been developed. As stated earlier, the procedure is applicable to shells of revolution with sharp discontinuities in geometry. The solution is well adapted to thick-walled pressure vessels since shearing deformations are included. However, the following note of caution regarding the use of these refined elements in elastic-plastic analysis should be made:

The result of an elastic-plastic analysis is primarily dependent on the number of integration points and their location. This information is used in the evaluation of Eq. (3-10). The number of points needed is almost independent of the kinematics of the element selected. For solid elements it is not feasible to obtain a relationship between strains and stress resultants by integration across the thickness. Therefore the matrix multiplications in Eq. (3-10) must be made at each integration point. By reducing the number of degrees of freedom per element, the number of numerical operations per integration point can be substantially reduced. Therefore the use of highly refined elements usually is not an optimum choice. For example, it may be more economical to use a larger number of elements of type (NP8-2) than a relatively few elements of type (NP10).

ACKNOWLEDGEMENTS

The authors are grateful to Professor E. L. Wilson of the University of California, Berkeley, for advice and encouragement.

REFERENCES

[1] Ergatoudis, I., Irons, B. M., and Zienkiewicz, O. C.: "Curved, Isoparametric, 'Quadrilateral' Elements for Finite Element Analysis," Int. J. Solids and Structures, vol. 4, 1968.

[2] Zienkiewicz, O. C., Irons, B. M., Ergatoudis, J., Ahmad, S., and Scott, F. C., "Iso-Parametric and Associated Element Families for Two- and Three-Dimensional Analysis," Finite Element Methods in Stress Analysis, ed. Holand, I., and Bell, K., Tapir, Trondheim, Norway, 1969.

[3] Doherty, W. P., Wilson, E. L., and Taylor, R. L., "Stress Analysis of Axisymmetric Solids Utilizing Higher-Order Quadrilateral Finite Elements," Report SESM 69-3, Dept. of Civil Engineering, University of California, Berkeley, 1969.

[4] Wilson, E. L., "SAP, A General Structural Analysis Program," Report UCSESM 70-20, Dept. of Civil Engineering, University of California, Berkeley, 1970.

[5] Hill, R., "The Mathematical Theory of Plasticity," Clarendon Press, Oxford, 1950.

[6] Khojasteh-Bakht, M., "Analysis of Elastic-Plastic Shells of Revolution under Axisymmetric Loading by the Finite Element Method," Ph.D. dissertation, Report SESM 67-8, Dept. of Civil Engineering, University of California, Berkeley, 1967 (available as NASA Report CR-85735).

[7] Prager, W., and Hodge, P. G., "Theory of Perfectly Plastic Solids," Dover Publications, Inc., 1968.

APPENDIX A. INTERPOLATION POLYNOMIALS

The following interpolation polynomials have been used.

Element (NP8-1)

$$\varphi_1 = \frac{1}{32}(1 + \eta)(1 - \xi)(-1 + 9\xi^2)$$

$$\varphi_2 = \frac{1}{32}(1 - \eta)(1 - \xi)(-1 + 9\xi^2)$$

$$\varphi_3 = \frac{9}{32}(1 + \eta)(1 - 3\xi)(1 - \xi^2)$$

$$\varphi_4 = \frac{9}{32}(1 - \eta)(1 - 3\xi)(1 - \xi^2)$$

$$\varphi_5 = \frac{9}{32}(1 + \eta)(1 + 3\xi)(1 - \xi^2)$$

$$\varphi_6 = \frac{9}{32}(1 - \eta)(1 + 3\xi)(1 - \xi^2)$$

$$\varphi_7 = \frac{1}{32}(1 + \eta)(1 + \xi)(-1 + 9\xi^2)$$

$$\varphi_8 = \frac{1}{32}(1 - \eta)(1 + \xi)(-1 + 9\xi^2)$$

Element (NP8-2)

$$\varphi_1 = \frac{1}{4}(1 + \eta)(1 - \xi)(-1 + \eta - \xi)$$

$$\varphi_2 = \frac{1}{2}(1 - \eta^2)(1 - \xi)$$

$$\varphi_3 = \frac{1}{4}(1 - \eta)(1 - \xi)(-1 - \eta - \xi)$$

$$\varphi_4 = \frac{1}{2}(1 - \xi^2)(1 + \eta)$$

$$\varphi_5 = \frac{1}{2}(1 - \xi^2)(1 - \eta)$$

$$\varphi_6 = \frac{1}{4}(1 + \eta)(1 + \xi)(-1 + \eta + \xi)$$

$$\varphi_7 = \frac{1}{2}(1 + \xi)(1 - \eta^2)$$

$$\varphi_8 = \frac{1}{4}(1 - \eta)(1 + \xi)(-1 - \eta + \xi)$$

Element (NP8-3)

As element (NP8-1) except for the added polynomial

$$\varphi_9 = \frac{1}{2}(1 - \eta^2)$$

Element (NP9-1)

$$\varphi_1 = \frac{1}{32}(\xi - 1)\{9(1 - \xi^2) + \eta(1 - 9\xi^2) - 8\eta^2\}$$

$$\varphi_2 = \frac{1}{32}(\xi - 1)\{9(1 - \xi^2) - \eta(1 - 9\xi^2) - 8\eta^2\}$$

$$\varphi_3 = \frac{9}{32}(1 - 3\xi)(1 - \xi^2)(1 + \eta)$$

$$\varphi_4 = \frac{9}{32}(1 - 3\xi)(1 - \xi^2)(1 - \eta)$$

$$\varphi_5 = \frac{9}{32}(1 + 3\xi)(1 - \xi^2)(1 + \eta)$$

$$\varphi_6 = \frac{9}{32}(1 + 3\xi)(1 - \xi^2)(1 - \eta)$$

$$\varphi_7 = \frac{1}{32}(1 + \xi)(1 + \eta)(9\xi^2 - 1)$$

$$\varphi_8 = \frac{1}{32}(1 + \xi)(1 - \eta)(9\xi^2 - 1)$$

$$\varphi_9 = \frac{1}{2}(1 - \xi)(1 - \eta^2)$$

Element (NP9-2)

$$\varphi_1 = \frac{1}{32}(1 - \xi)(9\xi^2 - 1)(1 + \eta)$$

$$\varphi_2 = \frac{1}{32}(1 - \xi)(9\xi^2 - 1)(1 - \eta)$$

$$\varphi_3 = \frac{9}{32}(1 - 3\xi)(1 - \xi^2)(1 + \eta)$$

$$\varphi_4 = \frac{9}{32}(1 - 3\xi)(1 - \xi^2)(1 - \eta)$$

Element (NP9-2) (cont.)

$$\varphi_5 = \frac{9}{32}(1 + 3\xi)(1 - \xi^2)(1 + \eta)$$

$$\varphi_6 = \frac{9}{32}(1 + 3\xi)(1 - \xi^2)(1 - \eta)$$

$$\varphi_7 = \frac{1}{32}(1 + \xi)\{-9(1 - \xi^2) - \eta(1 - 9\xi^2) + 8\eta^2\}$$

$$\varphi_8 = \frac{1}{32}(1 + \xi)\{-9(1 - \xi^2) + \eta(1 - 9\xi^2) + 8\eta^2\}$$

$$\varphi_9 = \frac{1}{2}(1 + \xi)(1 - \eta^2)$$

Element (NP10)

As element (NP9-1) except for

$$\varphi_7 = \frac{1}{32}(1 + \xi)\{-9(1 - \xi^2) - \eta(1 - 9\xi^2) + 8\eta^2\}$$

$$\varphi_8 = \frac{1}{32}(1 + \xi)\{-9(1 - \xi^2) + \eta(1 - 9\xi^2) + 8\eta^2\}$$

$$\varphi_9 = \frac{1}{2}(1 - \xi)(1 - \eta^2)$$

$$\varphi_{10} = \frac{1}{2}(1 + \xi)(1 - \eta^2)$$

Nodal Point Coordinates

The corner points for all elements have the coordinates $\xi = \pm 1$ and $\eta = \pm 1$. The midside points in (NP8-2) have $\xi = \pm 1$ and $\eta = 0$ and $\xi = 0$ and $\eta = \pm 1$. In the remaining elements the nodes on sides $\eta = \pm 1$ have coordinates $\xi = \pm 1/3$. The 9th nodal point in (NP9-1) and (NP9-2) is given by $\xi = -1$, $\eta = 0$, and $\xi = +1$, $\eta = 0$, respectively.

APPENDIX B. DERIVATION OF STIFFNESS MATRIX

The geometry and displacement field of the element is given by Eqs. (2-2) and (2-3)

$$\begin{Bmatrix} r \\ z \end{Bmatrix} = \sum_{i=1}^{N} \varphi_i(\xi,\eta) \begin{Bmatrix} r_i \\ z_i \end{Bmatrix} \tag{2-2}$$

$$\begin{Bmatrix} u \\ v \end{Bmatrix} = \sum_{i-1}^{N} \varphi_i(\xi,\eta) \begin{Bmatrix} u_i \\ v_i \end{Bmatrix} \tag{2-3}$$

For small displacement analysis of axisymmetric deformation the strain-displacement relations are given by

$$\begin{Bmatrix} \epsilon_r \\ \epsilon_z \\ \epsilon_\theta \\ \partial_{rz} \end{Bmatrix} = \begin{Bmatrix} \frac{\partial u}{\partial r} \\ \frac{\partial v}{\partial z} \\ \frac{u}{r} \\ \frac{\partial u}{\partial z} + \frac{\partial v}{\partial r} \end{Bmatrix} \tag{B-1}$$

In order to evaluate Eq. (B-1) the chain rule of differentiation has to be inverted to give

$$\begin{Bmatrix} \frac{\partial}{\partial r} \\ \frac{\partial}{\partial z} \end{Bmatrix} = \frac{1}{\det J} [J] \begin{Bmatrix} \frac{\partial}{\partial \xi} \\ \frac{\partial}{\partial \eta} \end{Bmatrix} \tag{B-2}$$

where $[J]$ is the Jacobian of the transformation (2-2), and is given by

$$[J] = \begin{bmatrix} \frac{\partial z}{\partial \eta} & -\frac{\partial z}{\partial \xi} \\ -\frac{\partial r}{\partial \eta} & \frac{\partial r}{\partial \xi} \end{bmatrix} \tag{B-3}$$

$$|J| = \det J = \frac{\partial z}{\partial \eta}\ \frac{\partial r}{\partial \xi} - \frac{\partial z}{\partial \xi}\ \frac{\partial r}{\partial \eta} \tag{B-4}$$

Using (2-2), (2-3) and (B-2), Eq. (B-4) can be evaluated

$$|J| = \varphi_{i,\xi} r_i \varphi_{j,\eta} z_j - \varphi_{i,\eta} r_i \varphi_{j,\xi} z_j = r_i (\varphi_{i,\xi}\varphi_{j,\eta} - \varphi_{i,\eta}\varphi_{j,\xi}) z_j \qquad i,j = 1,N$$

Let

$$[P] = \varphi_{i,\xi}\varphi_{j,\eta} - \varphi_{i,\eta}\,\varphi_{j,\xi} \tag{B-5}$$

$$|J| = \langle r \rangle [P] \{z\} \tag{B-6}$$

The strain component ϵ_r is found by

$$\epsilon_r = \frac{\partial u}{\partial r} = \frac{1}{|J|}\left(\frac{\partial z}{\partial \eta}\ \frac{\partial u}{\partial \xi} - \frac{\partial z}{\partial \xi}\ \frac{\partial u}{\partial \eta}\right) = \frac{1}{|J|}\ (\varphi_{i,\xi} u_i \varphi_{j,\eta} z_j - \varphi_{i,\eta} u_i \varphi_{j,\xi} z_j)$$

$$\epsilon_r = \frac{1}{|J|}\ u_i (\varphi_{i,\xi}\varphi_{j,\eta} - \varphi_{i,\eta}\varphi_{j,\xi}) z_j = \frac{1}{|J|}\ \langle u \rangle [P] \{z\} \tag{B-7}$$

Define

$$\{Y\} = \frac{1}{|J|}\ [P] \{z\}$$

$$\{Y\} = \frac{1}{|J|}\ \langle r \rangle [P] \tag{B-8}$$

$$\{G\} = \frac{\varphi_i}{r}$$

Following the procedure for ϵ_r the total strain-displacement relationship can be written

$$\begin{Bmatrix} \varepsilon_r \\ \varepsilon_z \\ \varepsilon_\theta \\ \partial_{rz} \end{Bmatrix} = \begin{bmatrix} Y_1 & 0 & Y_2 & 0 & & Y_N & 0 \\ 0 & X_1 & 0 & X_2 & & 0 & X_N \\ G_1 & 0 & G_2 & 0 & & G_N & 0 \\ X_1 & Y_1 & X_2 & Y_2 & & X_N & Y_N \end{bmatrix} \begin{Bmatrix} u_1 \\ v_1 \\ \cdot \\ \cdot \\ \cdot \\ u_N \\ v_N \end{Bmatrix}$$

or

$$\{\varepsilon\} = [B]\ \{u\} \tag{B-9}$$

Using the principle of virtual work the well known expression for the stiffness matrix is obtained.

$$[K] = 2\pi \int_{-1}^{+1} \int_{-1}^{+1} [B(\xi,\eta)]^T [C]\ [B(\xi,\eta)] \cdot r(\xi,\eta) \cdot |J|\, d\eta d\xi \tag{B-10}$$

The evaluation of Eq. (B-10) is done numerically using Gaussian quadrature. It should be noted that the selection of number of integration points is primarily dependent on the degree of accuracy needed in the determination of elastic-plastic zones within the element.

APPENDIX C. COMPUTER PROGRAM INPUT

This appendix gives a brief description of the input format for the program. A more detailed discussion of the program capabilities, storage requirements, etc., is contained in Appendix D.

Card No. 1. Control Card (I5)

Column 1-5: Number of independent structures to be analyzed in one run (NUMSTR)

Card No. 2. Title Card (72H)

Column 2-72: Alphanumeric information to be printed in the output heading

Card No. 3. Control Card (9I5)

Column 1-5: Number of nodal points (NUMNP)

" 6-10: Number of elements (NUMEL)

" 11-15: Number of points where boundary conditions are applied (NUMBC) (max. 40 points)

" 16-20: Problem index (IPLANE)
(IPLANE = 0, axisymmetric problem)
(IPLANE = 1, plane stress problem)

" 21-25: Number of pressure cards (NUMPC)

" 26-30: Number of load increments (NUMLI)

" 31-35: Number of nodes with applied concentrated loads or prescribed displacements (NUMCL)

" 36-40: Link index (NUMLE)
(NUMLE = 0, no interface with friction or discrete springs)

(NUMLE = 1, interface with friction or discrete springs present)

Column 41-45: Number of load increments before the friction or spring system is activated (MUMLE)

(If not needed leave blank.)

Card No. 4. Control Card (6I5)

Column 1-5: Integration index (INDX)

(INDX = 0, integration points given individually for each element)

(INDX = 1, same integration points for all elements)

" 6-10: Number of integration points in ξ-direction (NIX)

" 11-15: Number of integration points in η-direction (NIY)

(Leave Col. 6-15 blank if INDX = 0.)

" 16-20: Stress index (ISTR1)

(ISTR1 = 0, stresses not computed at **nodal** points)

(ISTR1 = 1, stresses computed at nodal points)

" 21-25: Stress index (ISTR2)

(ISTR2 = 1, nodal point stresses transformed to ξ-η coordinates)

" 26-30: Displacement index (IDISP)

(IDISP = 1, transform displacements to ξ-η coordinates)

Card No. 5. Nodal Point Data (2F20.10)

Column 1-20: r coordinate (XR)

" 21-40: z coordinate (XZ)

Total of NUMNP cards.

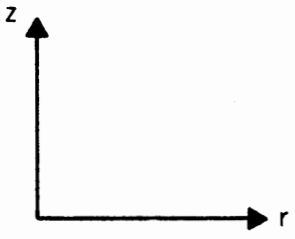

Card No. 6. Elastic Constants (E10.3, F5.3)

Column 1-10: Young's Modulus (E)

" 11-15: Poisson's ratio (u)

Card No. 7. Material Index (I5)

Column 1-5: Number of points describing the stress-strain relationship (NUMSP $\geq$ 2)

Card No. 8. Material Properties (2F10.5, E10.5)

Column 1-10: Strain at point i (ϵ_i)

" 11-20: Stress at point i (σ_i)

" 21-30: Tangent modulus at point i (Et_i)

Total of NUMSP cards. Point 1 has $\epsilon_1 = 0$, σ_1, Et_1

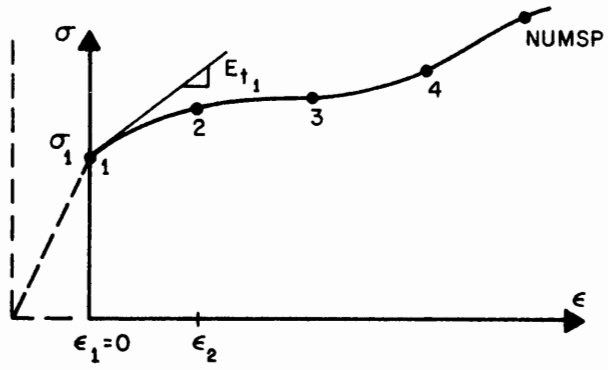

Card No. 9. Nodal Point Numbering (13I5)

Reference Fig. 1 for numbering sequence for each element type. Total of NUMEL cards.

Column 1-5: Nodal point 1

" 6-10: Nodal point 2

" 11-15: Nodal point 3

" 16-20: Nodal point 4

" 21-25 Nodal point 5

Column 26-30: Nodal point 6

" 31-35: Nodal point 7

" 36-40: Nodal point 8

" 41-45: Nodal point 9 (Blank for NP8-1, NP8-2)

" 46-50: Nodal point 10 (Only for NP10)

" 51-55: Element type (NTYPE)

NTYPE = 1 for NP8-1

NTYPE = 2 for NP8-2

NTYPE = 3 for NP9-1

NTYPE = 4 for NP9-2

NTYPE = 5 for NP10

" 56-60: Number of integration points in ξ-direction

" 61-65: Number of integration points in η-direction

(Col. 56-65 left blank if INDX = 1)

Card No. 10. Boundary Conditions (3I5, F10.5)

Column 1-5: Nodal point where B.C. are prescribed

" 6-10: Horizontal (or 1-direct.)

" 11-15: Vertical (or 2-direct.)

0 = Free
1 = Fixed
2 = Prescribed displacement

" 16-20: Angle in degrees for skew B.C. (α)

Total of NUMBC cards.

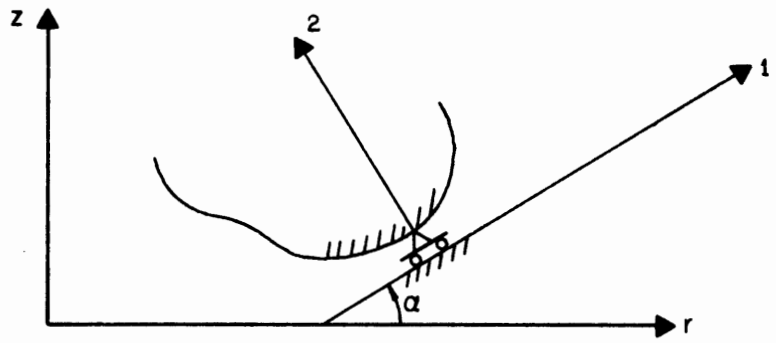

Card No. 11. Sliding Interfaces (2I5, F5.3)

This card should only be included if NUMLE ≠ 0.

Column 1-5: Number of element interfaces that can slide (NUMIF)

" 6-10: Interface index (INDF)

(INDF = 0, Coulomb's friction)

(INDF = 1, discrete springs or idealized friction)

" 11-15: Coefficient of friction (XMU)

Card No. 12. Nodal Points (8I5)

This card should only be included if NUMLE ≠ 0.

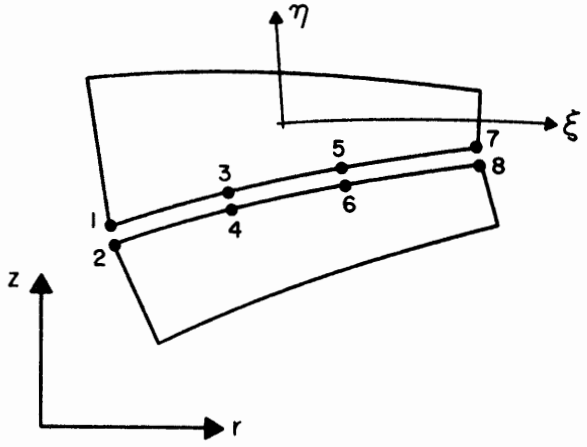

Column 1-5: Nodal point 1

" 6-10: Nodal point 2

" 11-15: Nodal point 3

" 16-20: Nodal point 4

" 21-25: Nodal point 5

" 26-30: Nodal point 6

" 31-35: Nodal point 7

" 36-40: Nodal point 8

(Column 31-40 left blank if element NP8-2 is used)

Total of NUMIF cards.

Card No. 13. Discrete Springs (8E10.5)

This card should only be included if NUMLE ≠ 0 and INDF = 1.

Total of NUMIF cards.

Column 1-10: Elastic spring constant K_1 at node 1

" 11-20: Elastic spring constant K_2 at node 1

" 21-30: Elastic spring constant K_1 at node 2

Column 31-40: Elastic spring constant K_2 at node 2

etc.

(Column 65-80 left blank if element NP8-2 is used.)

K_1 = spring in η-direction

K_2 = spring in ξ-direction

Card No. 14. Spring Options (8I5)

This card should only be included if NUMLE ≠ 0 and INDF = 1.

Total of NUMIF cards.

Column 1-5: Linkage index in η-direction at node 1, (ISP)

" 6-10: Linkage index in ξ-direction at node 1, (IFC)

" 11-15: Linkage index in η-direction at node 2

" 16-20: Linkage index in ξ-direction at node 2

" 21-25: Linkage index in η-direction at node 3

" 26-30: Linkage index in ξ-direction at node 3

" 31-35: Linkage index in η-direction at node 4

" 36-40: Linkage index in ξ-direction at node 4

(Col. 31-40 left blank if element NP8-2 is used.)

ISP = 0; free to move in η-direction

ISP = 1; fixed in η-direction

ISP = 2; prescribed spring, can take tension

ISP = 3; prescribed spring, cannot take tension

IFC = 0; free to slide in ξ-direction

IFC = 1; fixed in ξ-direction

IFC = 2; prescribed spring, can take tension

IFC = 3; idealized friction

Card No. 15. Loading Card (I5)

Column 1-5: Loading index (LNDX)

LNDX = 0; pure incremental analysis

LNDX = 1; one-step iteration method

Card No. 16. Load Intensities (5I3, 8F8.3)

This card should only be included if NUMPC > 0.

Total of NUMPC cards.

Column 1-3: Load index (ILOAD)

ILOAD = 0; horizontal and vertical load

ILOAD = 1; tangential and normal load

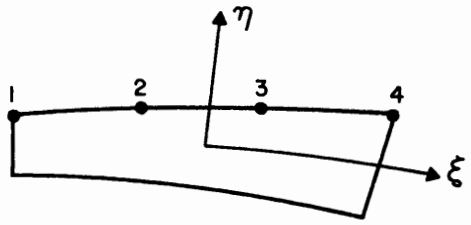

" 4-6: Nodal point 1

" 7-9: Nodal point 2

" 10-12: Nodal point 3

" 13-15: Nodal point 4

" 16-23: Horiz. (tang.) load intensity at node 1

" 24-31: Vert. (norm.) load intensity at node 1

" 32-39: Horiz. (tang.) load intensity at node 2

" 40-47: Vert. (norm.) load intensity at node 2

" 48-55: Horiz. (tang.) load intensity at node 3

" 56-63: Vert. (norm.) load intensity at node 3

" 64-71: Horiz. (tang.) load intensity at node 4

" 72-80: Vert. (norm.) load intensity at node 4

(Col. 13-15 and 64-80 left blank if element NP8-2 is used.)

Card No. 17. Concentrated Nodal Loads (I5, 2E15.8)

This card should only be included if NUMCL > 0.

Total of NUMCL cards.

Column 1-5: Node with concentrated load or prescribed displacement

" 6-15: Horizontal load X radius, or displacement

" 16-25: Vertical load X radius, or displacement

If the displacements are prescribed along skew boundary, they should be given in direction 1 and 2, respectively. See Card No. 10.

NOTE: For axisymmetric problems the nodal loads given above are the actual load per unit length, multiplied by the radial coordinate of the nodal point.

Card No. 18. Load Factor (8F10.5)

Total number of NUMLI/8 cards.

Column 1-10: Load proportionality factor for step 1 (DCOF)

" 11-20: Load proportionality factor for step 2

etc.

APPENDIX D. REMARKS ON THE USE OF THE PROGRAM

1. Output Information

The program prints the following output:

i) Input data

ii) Nodal point loads computed from load intensities

iii) Displacement increments and total displacements in global coordinates

iv) Total displacements in ξ-η coordinates (if wanted)

v) Stress distribution at integration points

vi) Stress distribution at nodal points (if wanted)

vii) Total stresses at nodal points in ξ-η coordinates (if wanted)

2. Size Limitations

The core storage requirements are separated into a fixed and a variable part. The fixed part consists of instructions, non-subscripted variables and arrays independent of the size of each individual problem. The variable part consists of the array A which appears in blank COMMON. The maximum dimension of A is limited to the number MTOT, which for a machine with 64 K storage equals 31000_{10}.

The capacity of the program is simply governed by the field length given on the job card. If this number implies a variable storage less that MTOT, the blank COMMON will be truncated accordingly.

For the binary version the fixed storage requirement is approximately 42000_8. The variable requirement (in decimal) is given by:

$$43 \times \text{NUMNP} + 13 \times \text{NUMEL} + 13 \times \text{NUMPC} + \text{NUMEQ} \times \text{NBNWD}$$

The last term in this sum is associated with the stiffness matrix, which is stored completely in core. An out-of-core equation-solver

could reduce the storage requirement substantially, but would on the other hand slow down the solution process.

3. Time

For elements with a large number of degrees of freedom the program is relatively slow, as pointed out in the conclusions. The time needed will be highly dependent on the number of integration points chosen, and engineering judgment should be used here. For most problems, the computer time used will be divided equally between the central and peripheral processor.

4. Additional Remarks on the Input

Card No. 4: The number MUMLE is given in order to be able to solve problems like shrink-fits. Here part of the structure is free to move indepently of the other during the first MUMLE load increments. From here on the linkage system is activated and the entire structure deforms as an integral unit.

Card No. 5: The coordinates of the corner points in each element can be chosen arbitrarily. The coordinates of the interior points, however, must be given according to the element type used. For all elements except (NP8-2), the nodes 3,5 and 4,6 trisect the element sides $\eta = +1$ and $\eta = -1$, respectively. The nodes 9 and 10 must bisect the element side $\xi = -1$ and $\xi = +1$. In element (NP8-2) all interior points are located at midside.

For elements with curved sides it may be difficult to determine the coordinates such that these requirements are

fulfilled. It should, however, be noted that the final results are dependent on how closely these requirements can be satisfied.

Card No. 4: Card No. 9 The number of integration points in either direction may be 2, 3, 4, 6, 8, 10, 12 or 16. For most cases 4 points are sufficient in the ξ-direction. The number needed in the η-direction depends on the element type used, and on whether an elastic or plastic analysis is performed. For elastic cases 2 points should be used for element NP8-1, and 3 points for all other elements (2 points here would give a singular stiffness matrix). For plastic analysis 6-8 points are usually sufficient, but engineering judgment should be used.

Card No. 18: The load level for each increment is governed by the load proportionality factor DCOF. This factor is given as a percentage of the total load previously given in the input. For a pure incremental analysis this factor should be given as load increment in percent of total load. If "out-of-balance force" method is used, the load factor should give the total load on the structure at any time.

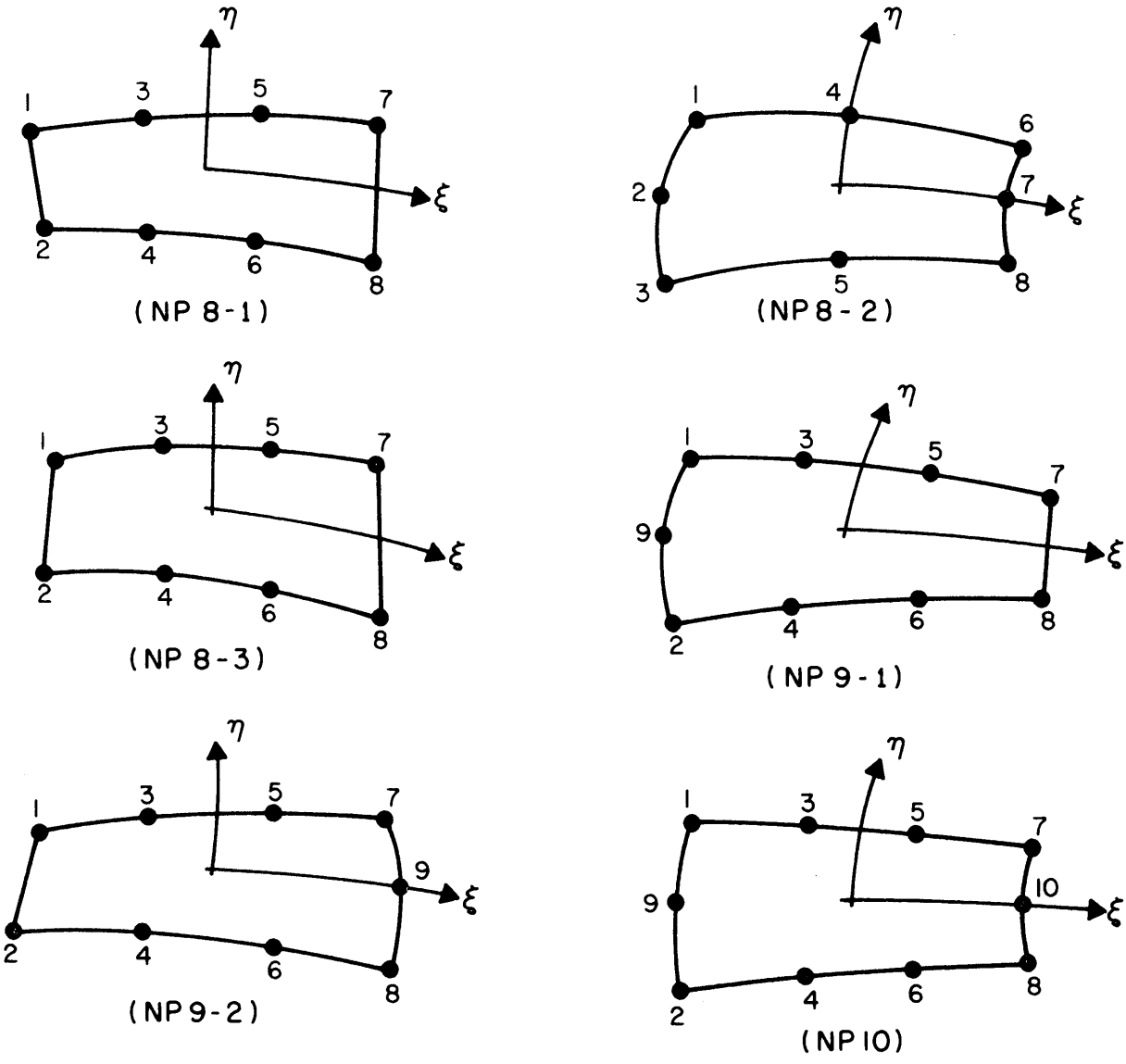

NOTE : (NP 8 - 3) HAS ONE INCOMPATIBLE DISPLACEMENT MODE ADDED

FIG. 1 ISOPARAMETRIC ELEMENTS

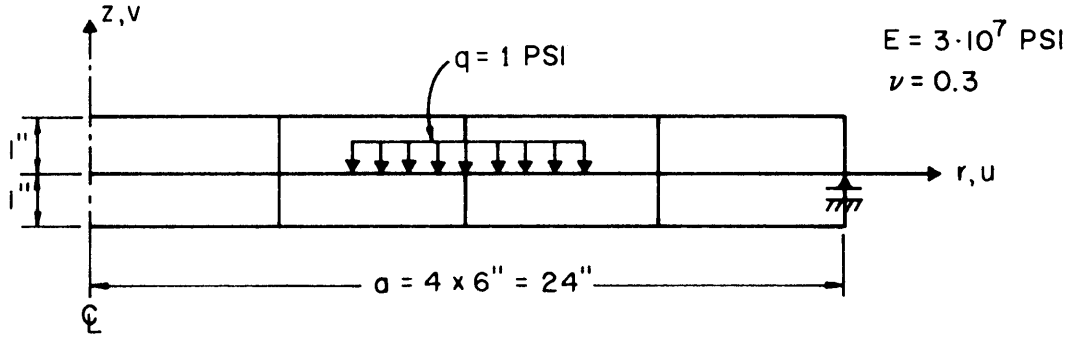

FIG. 2 CIRCULAR PLATE

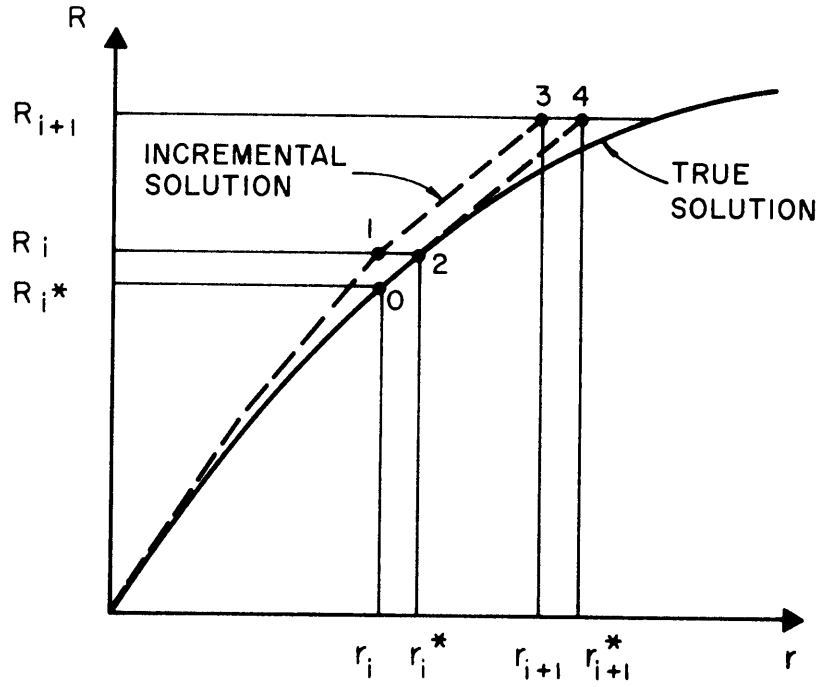

FIG. 3 SOLUTION METHOD

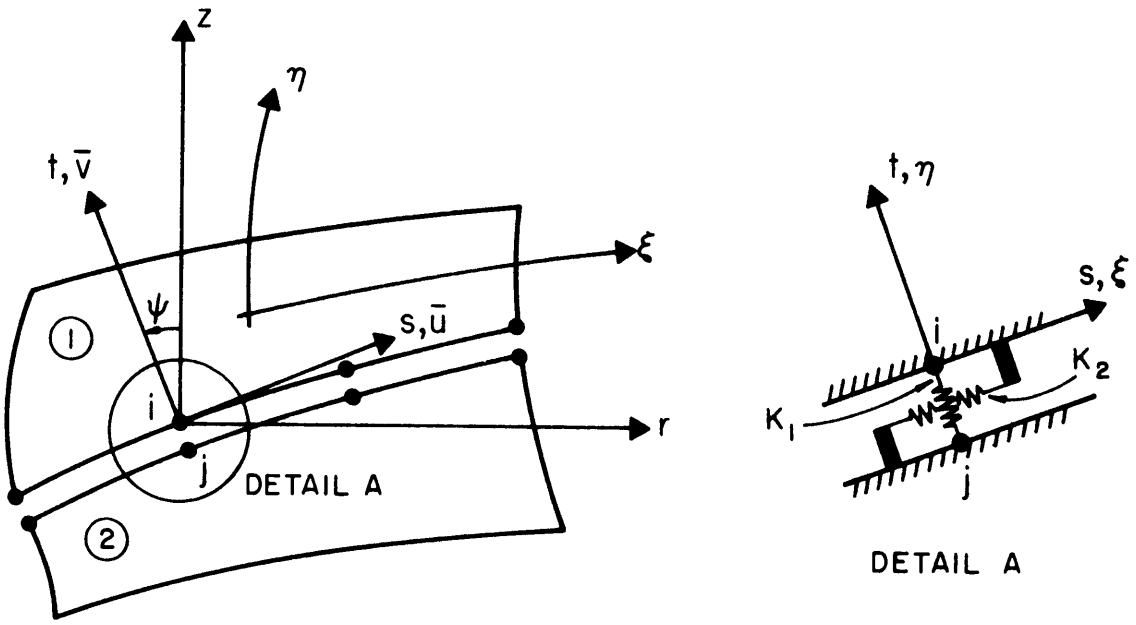

FIG. 4 SLIDING INTERFACE

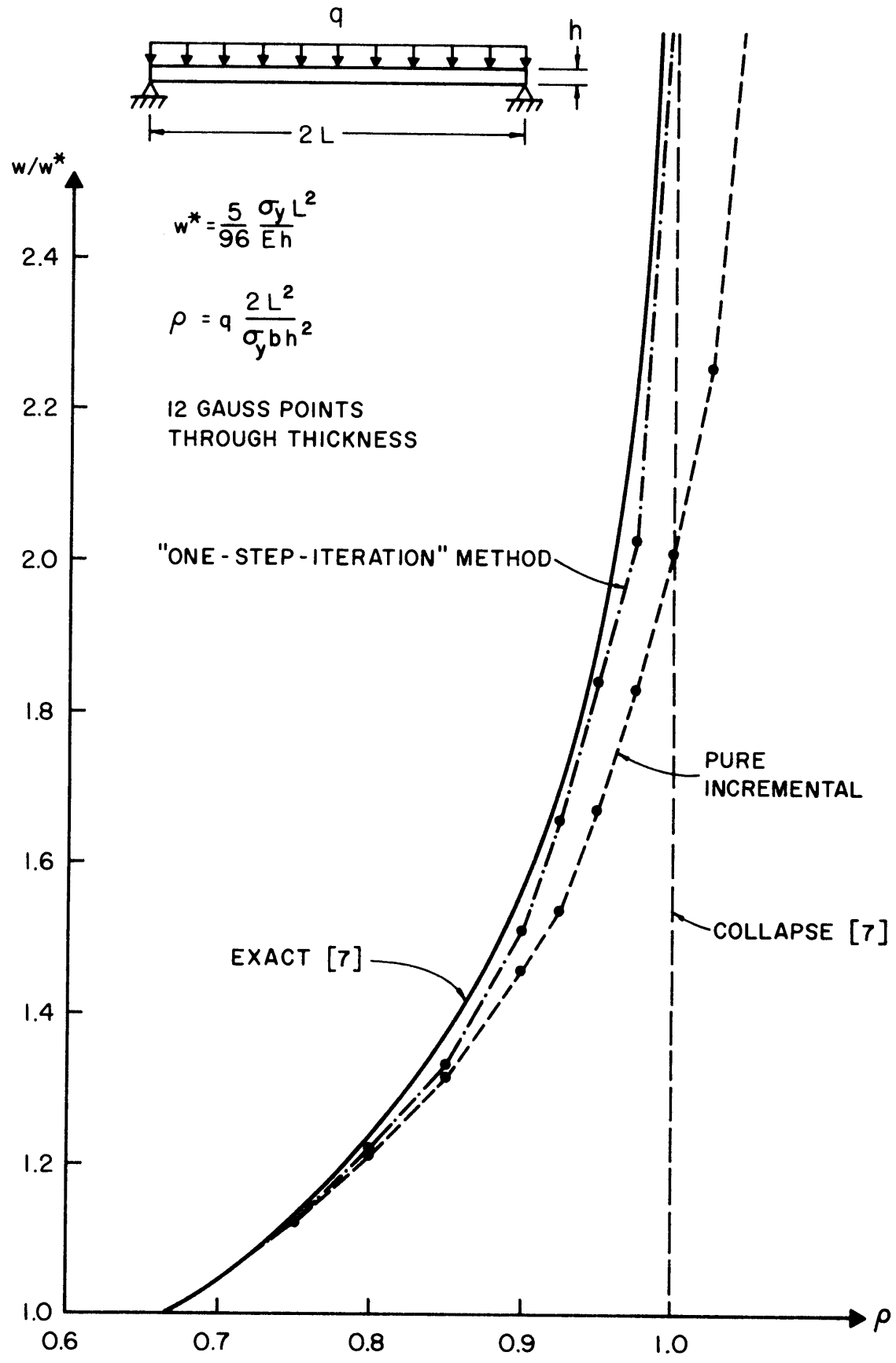

FIG. 5 ELASTIC-PLASTIC ANALYSIS OF BEAM

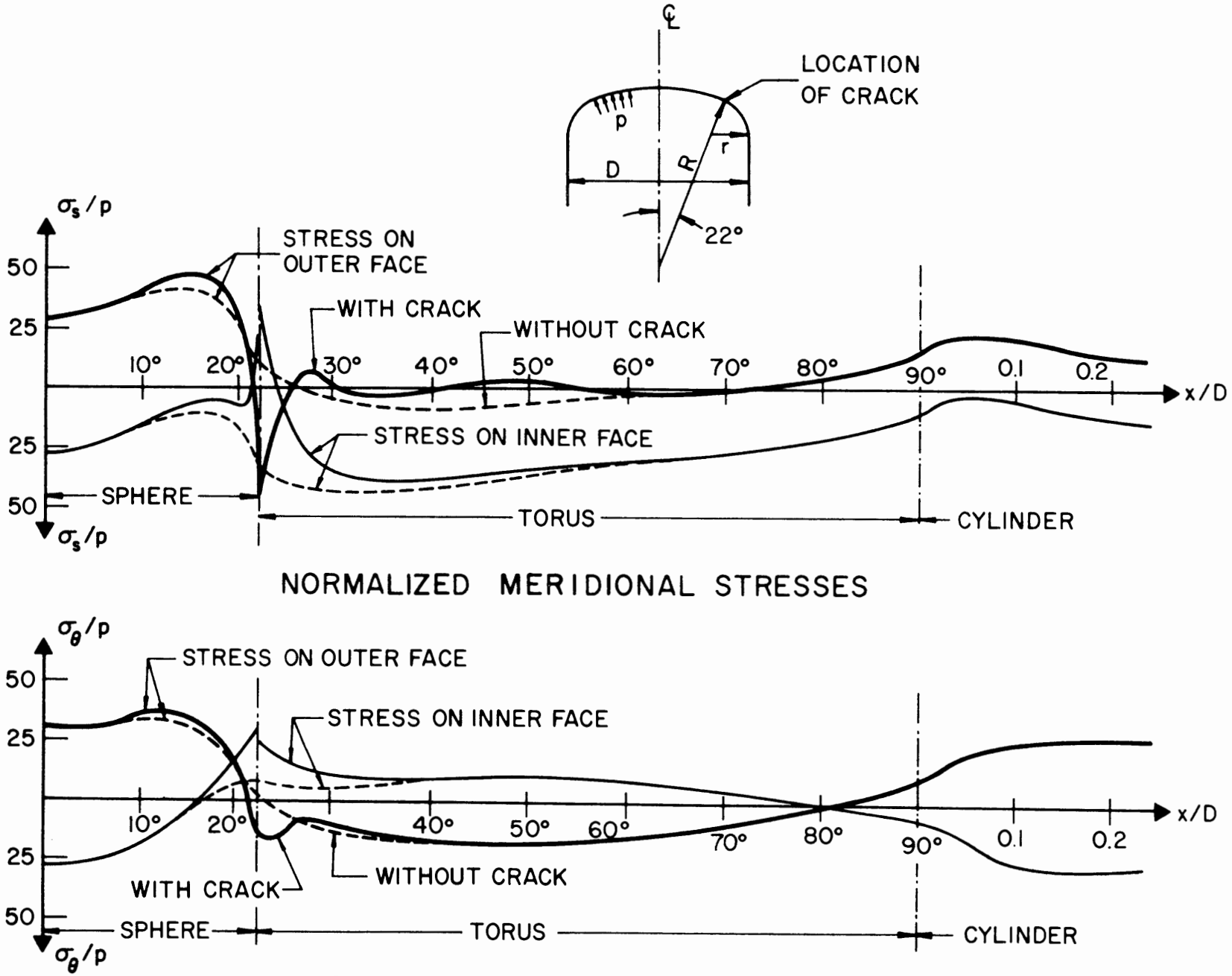

FIG. 6 ELASTIC STRESSES IN TORISPHERICAL HEAD

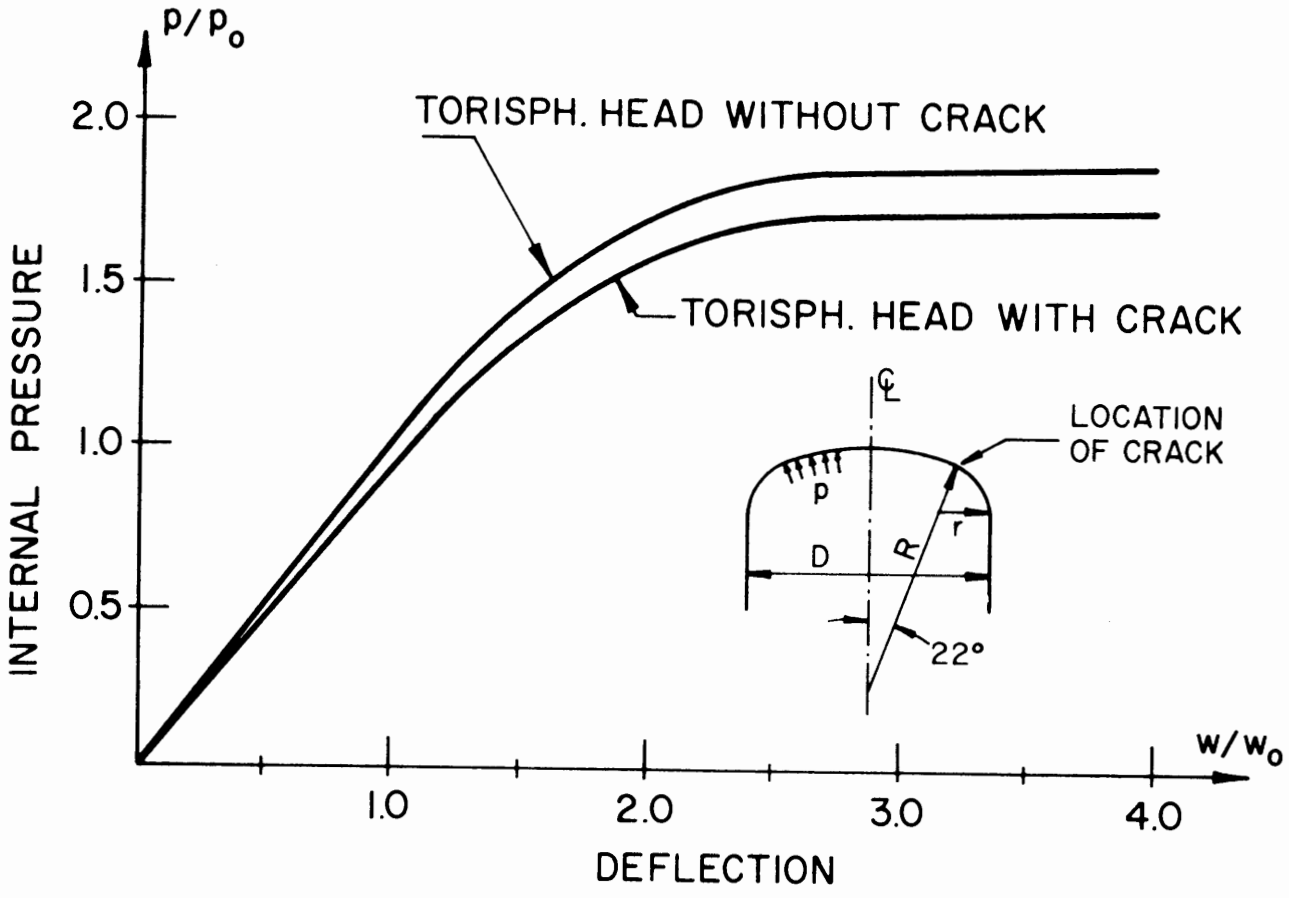

FIG. 7 DEFLECTION AT APEX

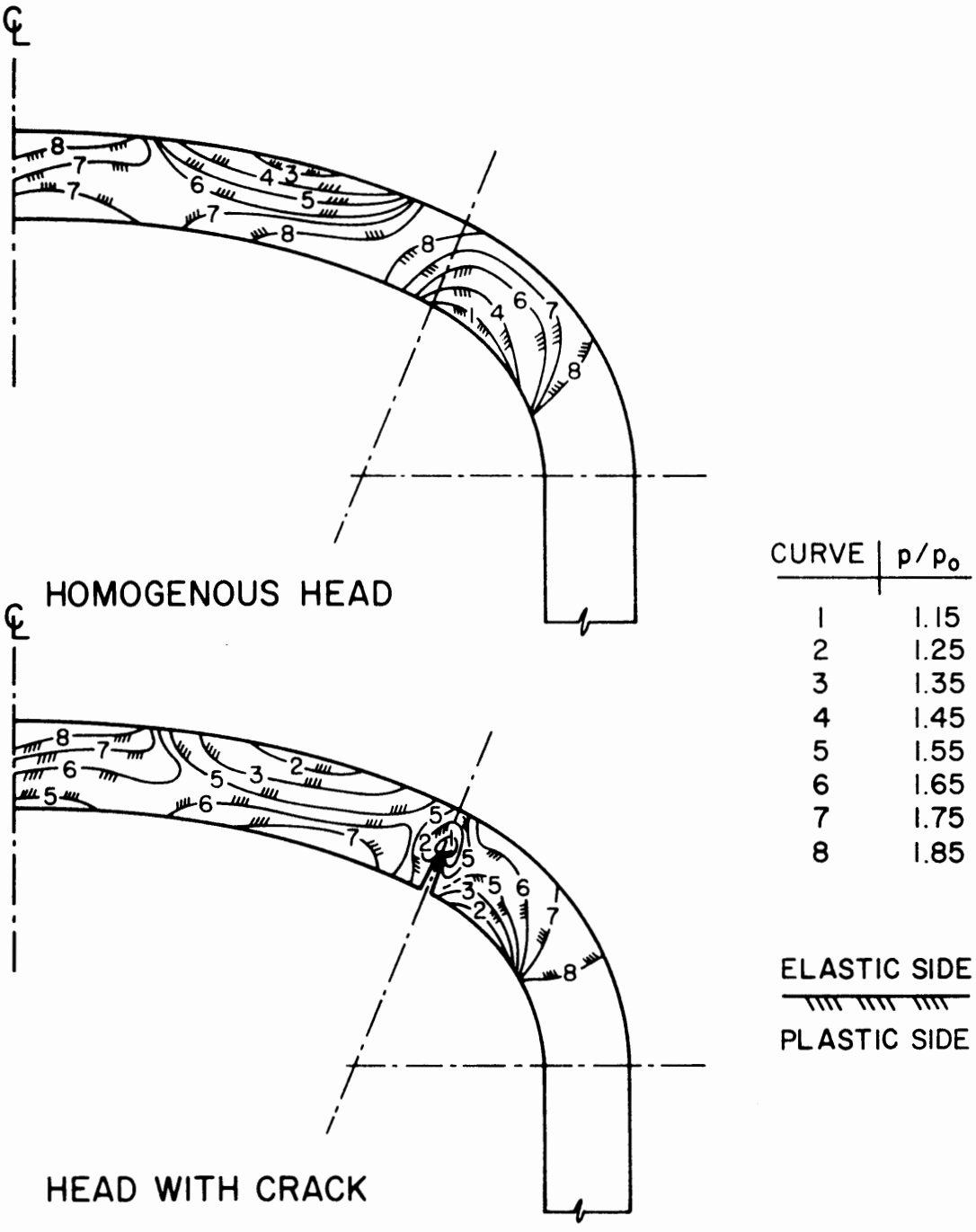

FIG. 8 ELASTIC-PLASTIC BOUNDARIES TORISPHERICAL HEAD

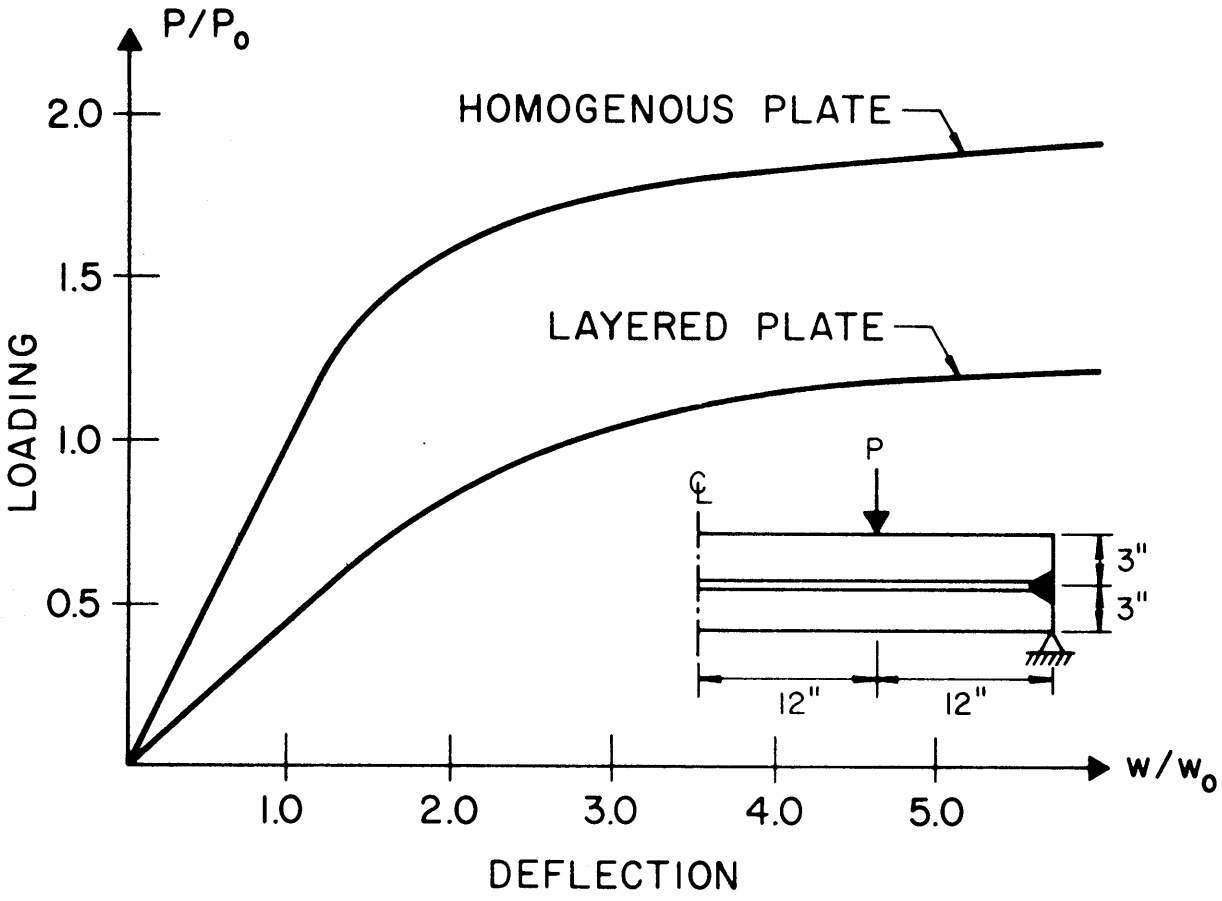

FIG. 10 CENTER DEFLECTION OF PLATE

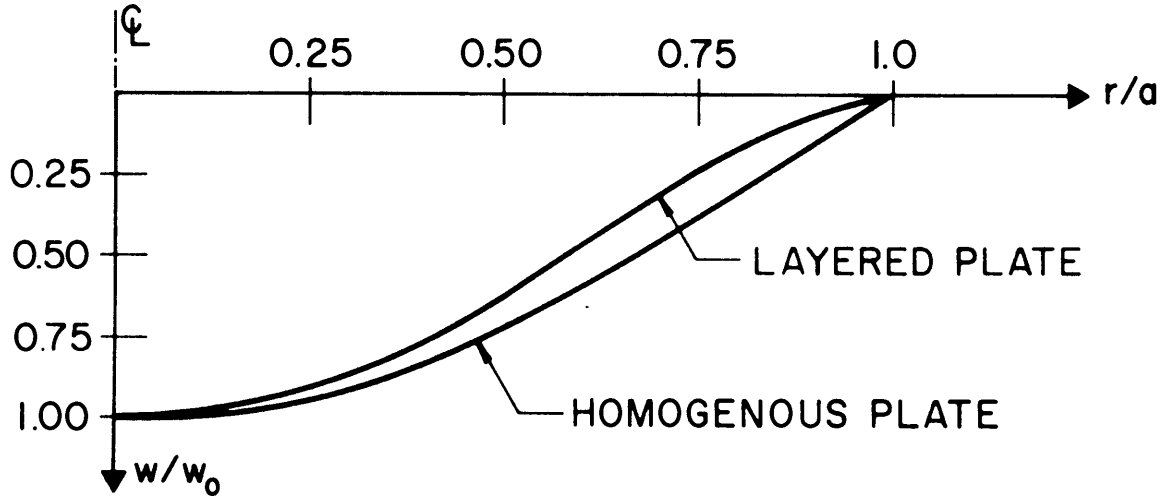

FIG. 9 DEFLECTION OF CIRCULAR PLATE

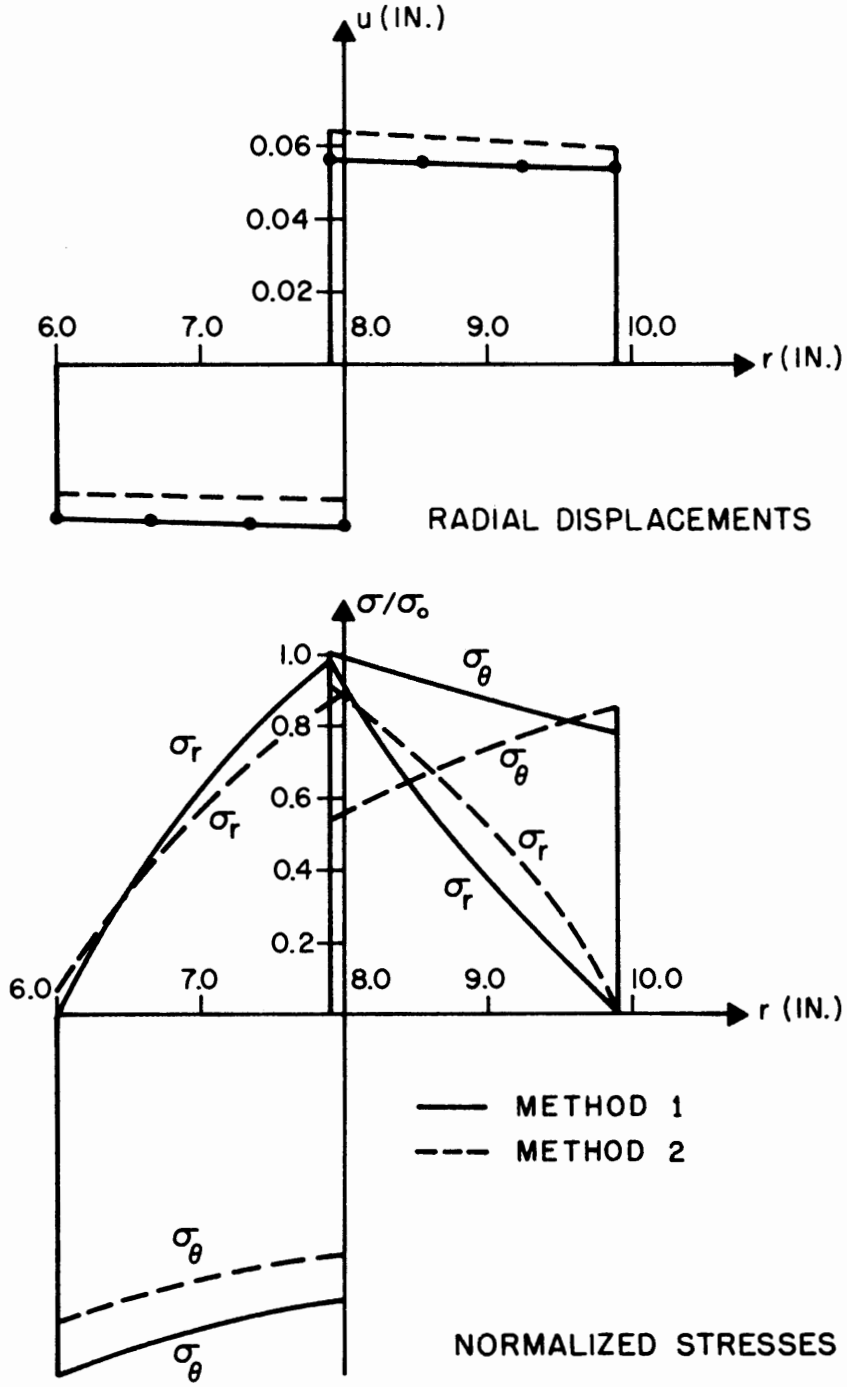

FIG.11 SHRINK-FIT OF TWO CYLINDRICAL THICKWALLED SLICES